Nonlinear Dyn (2022) 110:3823–3835
https://doi.org/10.1007/s11071-022-07813-9

ORIGINAL PAPER

Regulating memristive neuronal dynamical properties via excitatory or inhibitory magnetic field coupling

Zhenghui Wen · Chunhua Wang · Quanli Deng · Hairong Lin

Received: 29 April 2022 / Accepted: 27 July 2022 / Published online: 6 September 2022

Abstract The ion exchange in neurons can trigger time-varying magnetic fields. According to the superposition field principle, each neuron is exposed to the integrated magnetic field generated by the other neurons. This paper considers the effect of magnetic field coupling between two neurons on neuron dynamics. The magnetic flux of the memristor describes the impact of the magnetic field. According to the different coupling types of neurons, the excitatory coupling between excitatory neurons. The inhibitory magnetic coupling between excitatory and inhibitory neurons is also considered. And then, the excitatory and inhibitory magnetic field coupling is studied under different external excitation currents. The excitatory magnetic field coupling can promote the firing of neurons. When the intensity of inhibitory magnetic field coupling is large enough, the neuronal firing mode is static. The firing mode of neurons can be changed by adjusting the coupling intensity. Therefore, magnetic field coupling can provide new insights into the mechanism of information interaction between neurons. Finally, the excitability and inhibition of magnetic field coupling are improved by comparing magnetic field coupling with synaptic coupling. These results indicate that magnetic field coupling has the same function as a synapse to some extent and has the characteristics of radiation propagation.

Z. Wen · C. Wang (✉)· Q. Deng · H. Lin
College of Computer Science and Electronic Engineering, Hunan University, Changsha 410082, China
e-mail: wch1227164@hnu.edu.cn

Z. Wen
e-mail: wzhmaill@163.com

Keywords Magnetic field coupling · Inhibition and excitation · Electromagnetic induction · Hindmarsh–Rose neuron · Memristor

1 Introduction

The transmission of information between neurons is carried out by sequences of spikes [1]. The differential in the charged ions' concentration inside and outside the membrane determines a neuron's membrane potential. When a neuron transmits information, charged ions move in and out of the cell membrane to generate an action potential. According to the Maxwell electromagnetic induction theorem, the movement of charged ions can trigger time-varying electromagnetic fields [2]. The impact of magnetic fields on information transmission to neurons can help us better understand and explore life's mysteries.

The memristor is the fourth basic circuit element, representing the mathematical relationship between charge and flux [3]. Coexistence attractor [4–6], hidden attractor [7–9], hyperchaotic attractor [10–12], circular chaotic attractors [13], and other phenomena have been identified in the research of chaos based on memristor. Such complicated dynamics have been exploited to encrypt [14–16]. Memristors have been used in circuit elements to simulate biological synaptic functions [17–

19]. Various types of memristors were also being proposed [20], Fractional-order memristor [21–23], local active memristor [24–26], and so on.

Inspired by the magnetic flux physical characteristics of memristor [3], Ma et al. proposed introducing magnetic flux into the neuron model [27]. HR neuron model under electromagnetic radiation in 2016 to obtain a variety of discharge modes [28]. Based on this theory, the dynamic behaviors of different neuron models under electromagnetic radiation were explored [29–32]. For example, under the stimulation of electromagnetic radiation, FHN neurons can produce hidden extreme multistability phenomena [29]. Complex hidden cluster discharge patterns can be formed when the electromagnetic induction effect is applied to HR neurons [30]. The electrical activities of neurons under the electric fields were also considered in Refs. [31,32]. Introducing external electromagnetic radiation through an inductor coil, Ref. [33] proposed a new neuron model under the influence of time-varying electric and magnetic fields and external electromagnetic radiation. By introducing Hamiltonian energy to measure magnetic field energy, the relationship between different neuron discharge modes and energy under electromagnetic radiation was studied, such as HR neuron [34–36], FHN neuron [37,38], and Izhikevich neuron [39,40]. The researchers looked beyond the effects of electromagnetic radiation on neurons to neural networks. In Refs. [41–44], the chaotic dynamic behavior of the Hopfield neural network under the influence of external electromagnetic radiation on some neurons has been studied. The impact of different external stimuli on the chaotic dynamics of the Hopfield neural network was studied, and the energy transfer phenomenon of the neural network under other incentives was learned from the perspective of Hamiltonian energy [45]. The modulation of different kinds of external electromagnetic stimulation on the dynamics of the Newman–Watts small-world neural network model proved the feasibility of external electromagnetic stimulation in controlling the evolution of the neural network model [46].

Neurons communicate with one another via synapses [47,48]. Neurons may also receive input from inhibitory or excitatory postsynaptic potentials. The excitatory synapse can increase firing usually, and the inhibitory synapse makes possible a reduction in neuronal firing [49]. Sometimes, increased arrival rates of inhibitory input can enhance firing rates, and increased excitatory input rates can decrease firing rates [50]. Synapses in the neurological system are classified as electrical or chemical synapses [51]. Electrical synapses convey messages to postsynaptic neurons via electric currents. Chemical synapses transmit information via neurotransmitters, which either excite or inhibit postsynaptic neurons depending on the neurotransmitter. Chemical synapses are characterized by unidirectional transmission and delay because neurotransmitters can only pass from the presynaptic membrane to the postsynaptic membrane. It would be interesting to discover another efficient method of signaling communication between neurons. In [52], scholars studied magnetic field coupling, the interaction between neuron magnetic fields, and proposed the coupling neuron model. When magnetic field coupling and electrical synaptic coupling exist in neural networks, magnetic field coupling can regulate the collective behavior of neural networks [53,54]. In the case that magnetic field coupling, electric field coupling and synaptic coupling simultaneously act on the Newman–Watts small-world neuronal network, standard deviation and synchronization factors are introduced to provide helpful guidance for signal transmission between neurons [55]. The above studies suggest that magnetic field coupling is another way of neuron signal propagation. In [52–55], the influence of magnetic field coupling is considered. In [52,53], it is considered that magnetic field coupling promotes phase synchronization of neurons. In [54,55], Magnetic field coupling was considered to regulate neuron activity, but only excitatory neuron networks were considered.

However, it is a pity that the split of magnetic field coupling into excitatory and inhibitory magnetic field coupling was not considered in previous researches [52–55]. Excitatory and inhibitory synapses are two types of synapses [47]. As magnetic field coupling is another means of neuron signal communication, the regulation of inhibitory and excitatory magnetic field coupling on neuronal dynamical properties should also be considered. Based on the above discussion, this paper puts forward the concept of excitation and inhibition of magnetic field coupling and proposes the corresponding theoretical model. According to Abe's theorem, the direction of the magnetic field is determined by the law of ion movement. Therefore, the excitation and inhibition of neurons can be indicated by the direction of the magnetic field. The magnetic fields of the two neurons are superimposed on each other, either in the same direction or opposite. The excitatory magnetic field coupling and inhibitory magnetic field coupling models are proposed. It is verified that excitatory magnetic field coupling can promote the firing of neurons, inhibitory magnetic field coupling can inhibit the corresponding neuron, and the increasing coupling intensity to a certain degree makes the neuron reach the static state.

The following of this paper is organized as follows; Sect. 2 splits magnetic field coupling into excitatory and inhibitory magnetic field coupling; Sect. 3 studies two magnetic field coupling states under four discharge modes; Sect. 4 summarizes the full text.

2 Model description and scheme considered

Synapses are the connections between neurons. And the importance of magnetic coupling as a possible way of transmitting information between neurons is undeniable. To study the modulation of dynamical properties of coupling neurons by excitatory and inhibitory magnetic field coupling. In this paper, we consider the response of the magnetic field coupled HR model to external stimulus currents in two cases: Case I. Excitatory magnetic field coupling model; Case II. Inhibitory magnetic field coupling model.

2.1 Excitatory magnetic field coupling model

In [52], a model of interaction between neuron magnetic fields was presented. In Refs. [53,55,56], electrical synapses and magnetic fields were used for information interaction between neurons. And the two neurons connected by magnetic coupling were both excited, so it can be considered that the magnetic coupling connecting the two excited neurons is also excitatory magnetic coupling. The corresponding excitatory magnetic field coupling model is shown below:

$$\begin{cases} \dot{x}_1 = y_1 - a{x_1}^3 + b{x_1}^2 - z_1 + I_{\text{ext}} - k\rho(\varphi_1)x_1 \\ \dot{y}_1 = c - d{x_1}^2 - y_1 \\ \dot{z}_1 = r[s(x_1 + 1.6) - z_1] \\ \dot{\varphi}_1 = k_1x_1 - k_2\varphi_1 + G_{\text{ex}}(\varphi_2 - \varphi_1) \\ \dot{x}_2 = y_2 - a{x_2}^3 + b{x_2}^2 - z_2 + I_{\text{ext}} - k\rho(\varphi_2)x_2 \\ \dot{y}_2 = c - d{x_2}^2 - y_2 \\ \dot{z}_2 = r[s(x_2 + 1.6) - z_2] \\ \dot{\varphi}_2 = k_1x_2 - k_2\varphi_2 + G_{\text{ex}}(\varphi_1 - \varphi_2), \end{cases} \tag{1}$$

where x, y, z and φ describe the membrane potential, recovery variables of slow current and adaptive current, and magnetic flux, respectively. I_{ext} is the external stimulus current, the memristor coupling magnetic flux and membrane potential. Its conductivity is $\rho(\varphi) = \alpha + 3\beta\varphi^2$. $G_{\text{ex}}(\varphi_1 - \varphi_2)$ and $G_{\text{ex}}(\varphi_2 - \varphi_1)$, represent the interaction of two magnetic fields. G_{ex} means the coupling strength of the corresponding excitatory magnetic field, and the other parameters (a, b, c, d, k, r, s, k_1, k_2) are constants as (1.0, 3.0, 1.0, 5.0, 1, 0.006, 4, 0.5, 0.5).

2.2 Inhibitory magnetic field coupling model

It is well known that synapses can be divided into inhibitory and excitatory. Inhibitory synapses connect the neurons, and the presynaptic neuron is activated while the postsynaptic neuron is inhibited. In this paper, magnetic field coupling is another way of neuron information transmission. Therefore, there is also a corresponding inhibitory magnetic field coupling. That is, the upper-level neuron is activated while the lower-level neuron is inhibited, and they communicate with one another via magnetic field coupling. In this work, we propose the inhibitory magnetic field model coupling two neurons as:

$$\begin{cases} \dot{x}_1 = y_1 - a{x_1}^3 + b{x_1}^2 - z_1 + I_{\text{ext}} - k\rho(\varphi_1)x_1 \\ \dot{y}_1 = c - d{x_1}^2 - y_1 \\ \dot{z}_1 = r[s(x_1 + 1.6) - z_1] \\ \dot{\varphi}_1 = k_1x_1 - k_2\varphi_1 - G_{\text{in}}(\varphi_2 + \varphi_1) \\ \dot{x}_2 = y_2 - a{x_2}^3 + b{x_2}^2 - z_2 + I_{\text{ext}} - k\rho(\varphi_2)x_2 \\ \dot{y}_2 = c - d{x_2}^2 - y_2 \\ \dot{z}_2 = r[s(x_2 + 1.6) - z_2] \\ \dot{\varphi}_2 = k_1x_2 - k_2\varphi_2 + G_{\text{in}}(\varphi_1 + \varphi_2), \end{cases} \tag{2}$$

where G_{in} is the coupling strength of the corresponding inhibitory magnetic field.

It is well known that adjusting the applied excitation current can alter the firing pattern of neurons. To explore the influence of different degrees of magnetic field coupling intensity on neuronal firing mode under other circumstances, we studied two magnetic field coupling cases with four different firing patterns, as shown in Table 1.

Table 1 Cases of different firing states according to magnetic field coupling types

Different states	Spiking firing $I_{\text{ext}} = 1.8$	Bursting firing $I_{\text{ext}} = 2.3$	Chaotic firing $I_{\text{ext}} = 3.2$	Periodical firing $I_{\text{ext}} = 4$
Excited-excited	Sec3.1-Case1	Sec3.1-Case2	Sec3.1-Case3	Sec3.1-Case4
Excited-inhibited	Sec3.2-Case1	Sec3.2-Case2	Sec3.2-Case3	Sec3.2-Case4

2.3 Stability analysis for the equilibrium states

The equilibrium Eq. (3) is found by zeroing the left side of Eq. (1)

$$\begin{cases} y_1 - a{x_1}^3 + b{x_1}^2 - z_1 + I_{\text{ext}} - k\rho(\varphi_1)x_1 = 0 \\ c - d{x_1}^2 - y_1 = 0 \\ r[s(x_1 + 1.6) - z_1] = 0 \\ k_1x_1 - k_2\varphi_1 + G_{\text{ex}}(\varphi_2 - \varphi_1) = 0 \\ y_2 - a{x_2}^3 + b{x_2}^2 - z_2 + I_{\text{ext}} - k\rho(\varphi_2)x_2 = 0 \\ c - d{x_2}^2 - y_2 = 0 \\ r[s(x_2 + 1.6) - z_2] = 0 \\ k_1x_2 - k_2\varphi_2 + G_{\text{ex}}(\varphi_1 - \varphi_2) = 0, \end{cases} \tag{3}$$

The equations may be solved using MATLAB, and the real solution is the equilibrium point. The following approach is used to construct the Jacobian matrix corresponding to Eq. (1).

$$J = \begin{pmatrix} J_{11} & 1 & -1 & J_{14} & 0 & 0 & 0 & 0 \\ J_{21} & -1 & 0 & 0 & 0 & 0 & 0 & 0 \\ J_{31} & 0 & J_{33} & 0 & 0 & 0 & 0 & 0 \\ J_{41} & 0 & 0 & J_{44} & 0 & 0 & 0 & J_{48} \\ 0 & 0 & 0 & 0 & J_{55} & 1 & -1 & J_{58} \\ 0 & 0 & 0 & 0 & J_{65} & -1 & 0 & 0 \\ 0 & 0 & 0 & 0 & J_{75} & 0 & J_{77} & 0 \\ 0 & 0 & 0 & J_{84} & J_{85} & 0 & 0 & J_{88} \end{pmatrix} \tag{4}$$

where

$$J_{11} = 2bx_1 - 3ax_1^2 - k(\alpha + 3\beta\varphi_1^2);\ J_{21} = -2dx_1;$$
$$J_{31} = J_{75} = rs;\ J_{85} = J_{41} = k_1;$$
$$J_{14} = -6k\beta\varphi_1x_1;\ J_{33} = J_{77} = -r;$$
$$J_{88} = J_{44} = -k_2 - G_{\text{ex}};\ J_{48} = J_{84} = G_{\text{ex}};$$
$$J_{55} = 2bx_2 - 3ax_2^2 - k(\alpha + 3\beta\varphi_2^2);\ J_{65} = -2dx_2;$$
$$J_{58} = -6k\beta\varphi_2x_2.$$

The eigenvalues of the appropriate equilibrium point are calculated by substituting it into the Jacobian matrix.

The related equilibrium Eq. (5) is found by zeroing the left side of Eq. (2).

$$\begin{cases} y_1 - a{x_1}^3 + b{x_1}^2 - z_1 + I_{\text{ext}} - k\rho(\varphi_1)x_1 = 0 \\ c - d{x_1}^2 - y_1 = 0 \\ r[s(x_1 + 1.6) - z_1] = 0 \\ k_1x_1 - k_2\varphi_1 - G_{\text{in}}(\varphi_2 + \varphi_1) = 0 \\ y_2 - a{x_2}^3 + b{x_2}^2 - z_2 + I_{\text{ext}} - k\rho(\varphi_2)x_2 = 0 \\ c - d{x_2}^2 - y_2 = 0 \\ r[s(x_2 + 1.6) - z_2] = 0 \\ k_1x_2 - k_2\varphi_2 + G_{\text{in}}(\varphi_1 + \varphi_2) = 0, \end{cases} \tag{5}$$

The Jacobian matrix of (2) is yielded as

$$J = \begin{pmatrix} J_{11} & 1 & -1 & J_{14} & 0 & 0 & 0 & 0 \\ J_{21} & -1 & 0 & 0 & 0 & 0 & 0 & 0 \\ J_{31} & 0 & J_{33} & 0 & 0 & 0 & 0 & 0 \\ J_{41} & 0 & 0 & J_{44} & 0 & 0 & 0 & J_{48} \\ 0 & 0 & 0 & 0 & J_{55} & 1 & -1 & J_{58} \\ 0 & 0 & 0 & 0 & J_{65} & -1 & 0 & 0 \\ 0 & 0 & 0 & 0 & J_{75} & 0 & J_{77} & 0 \\ 0 & 0 & 0 & J_{84} & J_{85} & 0 & 0 & J_{88} \end{pmatrix} \tag{6}$$

where

$$J_{11} = 2bx_1 - 3ax_1^2 - k(\alpha + 3\beta\varphi_1^2);\ J_{21} = -2dx_1;$$
$$J_{31} = J_{75} = rs;\ J_{85} = J_{41} = k_1;$$
$$J_{14} = -6k\beta\varphi_1x_1;\ J_{33} = J_{77} = -r;$$
$$J_{44} = -k_2 - G_{\text{in}};\ J_{48} = -G_{\text{in}};$$
$$J_{55} = 2bx_2 - 3ax_2^2 - k(\alpha + 3\beta\varphi_2^2);\ J_{65} = -2dx_2;$$
$$J_{58} = -6k\beta\varphi_2x_2;\ J_{84} = G_{\text{in}};\ J_{88} = -k_2 + G_{\text{in}}.$$

The equilibrium point of an actual number solution is first found by solving equations and then replaced into the Jacobian matrix, and the stability of the equilibrium point is determined by its eigenvalue. Table 2 summarizes the findings.

Neither excitatory nor inhibitory magnetic field coupling has an equilibrium point when G_{ex}=0 or $G_{\text{in}} = 0$. The applied excitation current determines the equilibrium point in excitatory magnetic field coupling. The

Table 2 Equilibrium points and their corresponding eigenvalues and stabilities ($I_{\text{ext}} = 3.2$)

Parameters	Equilibrium points	Eigenvalues	Stabilities
$G_{\text{ex}} = 0.2$	−0.6865, −1.3561, 3.6542, −1.3729, −0.6865, −1.3561, 3.6542, −1.3729	−6.8806, −6.8801, −0.8992, −0.4939, 0.1289, 0.1225, 0.0197, 0.0213	Unstable saddle point
$G_{\text{ex}} = 0.8$	−0.6865, −1.3561, 3.6542, −1.3729, −0.6865, −1.3561, 3.6542, −1.3729	−6.8806, −6.8783, −2.1052, 0.0213, −0.4939, 0.1342, 0.1225, 0.0187	Unstable saddle point
$G_{\text{ex}} = 2$	−0.6865, −1.3561, 3.6542, −1.3729, −0.6865, −1.3561, 3.6542, −1.3729	−6.8806, −6.8693, −4.5161, 0.0213, −0.4939, 0.1365, 0.1225, 0.0183	Unstable saddle point
$G_{\text{in}} = 0.2$	−0.7000, −1.4499, 3.6001, −0.3130, −0.6587, −1.1694, 3.7652, −2.4043	−6.9387, −6.7784, −0.6976±0.2024i, 0.1508, 0.0739, 0.0160, 0.0382	Unstable saddle-focus
$G_{\text{in}} = 0.8$	−0.6538, −1.1374, 3.7847, 2.5494, −0.5515, −0.5207, 4.1940, −4.9600	−6.7882, −6.5947, −1.3027±0.8024i, 0.1048, 0.0259, −0.0202±0.0582i	Unstable saddle-focus
$G_{\text{in}} = 1.4$	−0.5654, −0.5986, 4.1383, 4.6618, −0.4690, −0.0997, 4.5241, −6.7307	−6.6408, −6.7855, −1.9026±1.4007i, −0.1846, 0.0022±0.0597i, −0.0255	Unstable saddle-focus
$G_{\text{in}} = 1.5$	−0.5517, −0.5220, 4.1931, 4.9551, −0.4580, −0.0490, 4.5678, −6.9746	−6.6418, −6.8424, −2.0024±1.5005i, −0.2134, −0.0102±0.0601i, −0.0226	Stable focus-node
$G_{\text{in}} = 2$	−0.4913, −0.2067, 4.4350, 6.2435, −0.4120, 0.1513, 4.7520, −8.0501	−6.7493, −7.1999, −2.5013±1.9992i, −0.3363, −0.1025, −0.0430, −0.0159	Stable focus-node

excitatory magnetic field coupling intensity has a minor effect on the eigenvalue but no impact on the equilibrium point. The inhibitory magnetic field coupling intensity can affect both the equilibrium point and the eigenvalue in the inhibitory magnetic field coupling. The stability of the equilibrium point varies from unstable equilibrium point to stable equilibrium point as the magnetic field coupling strength increases.

3 Numerical results and discussion

In numerical study, this section uses the fourth order Runge–Kutta algorithm to solve the dynamic equation with a transient period of 1200. Neurons in the model of the initial value are set to $(x_1, y_1, z_1, \varphi_1, x_2, y_2, z_2, \varphi_2) = (0.2, 0.5, 0.1, 0.1, 0.3, 0.8, 0.2, 0.0)$, the other parameters are chosen as a=1.0, b=3.0, c=1.0, d=5.0, r=0.006, s=4, k=1, k_1=0.5, k_2=0.5, α=0.1, β=0.02. For clear illustration, the influence of applied current on the electrical activity of neurons can be illustrated by the inter-spike interval (ISI) bifurcation diagram as shown in Fig. 1.

ISI reflects the distance between two peaks in the firing sequence diagram of neurons. The firing modes of the HR neuronal models experienced several major transitions. When the external stimulus I_{ext} is too tiny, the neuron is in a quiescent state. With the increase of external stimulation, the neuron experiences spike discharge, burst discharge, chaotic discharge and periodic oscillation. We can select the appropriate external excitation current to control the firing mode of neurons, as shown in Fig. 2.

Various modes of electrical activity can be triggered by selecting the right applied excitation current. And two neurons with different initial values fired in the same pattern without synaptic coupling and magnetic

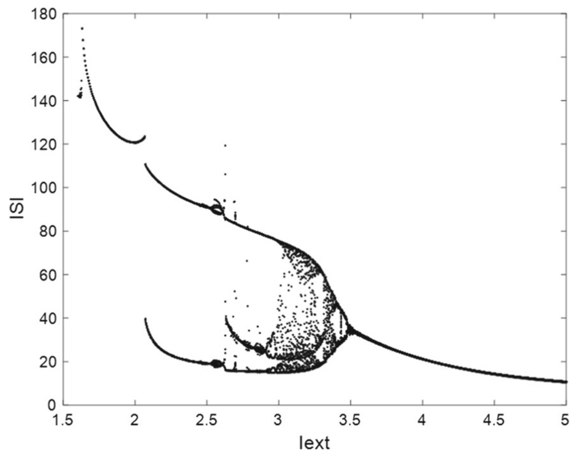

Fig. 1 Bifurcation diagram of neuron membrane potential and different external stimulus signals

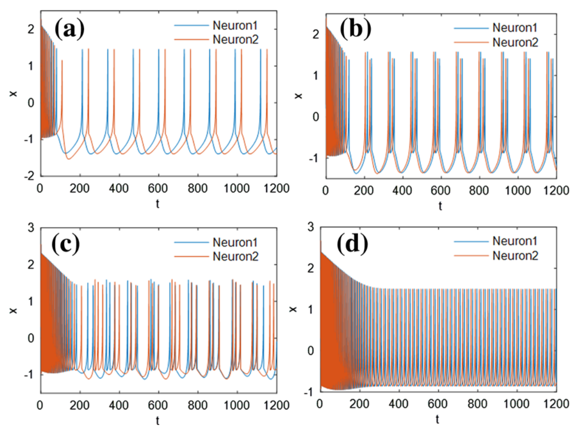

Fig. 2 Two neurons with different initial values were sampled with different excitation (the blue is the response of the first neuron, and the orange is the response of the second neuron). **a** $I_{\text{ext}} = 1.8$; **b** I_{ext} =2.3; **c** I_{ext} =3.2; **d** I_{ext} =4; The initial values are selected as (0.2, 0.5, 0.1, 0.1, 0.3, 0.8, 0.2, 0.0)

coupling. When the external excitation current is fixed, the regulation of excitatory and inhibitory magnetic field coupling on neuronal dynamical properties under different discharge modes is explored through bifurcation analysis of magnetic field coupling intensity.

3.1 Inhibitory magnetic field coupling

In case 1, two neurons with different initial values at peak discharge were selected to change the intensity of magnetic field coupling, and the effect of magnetic field coupling on neuron firing mode was detected. Bifurcation of ISI with parameter G_{in} and neuron firing patterns are shown in Figs. 3 and 4.

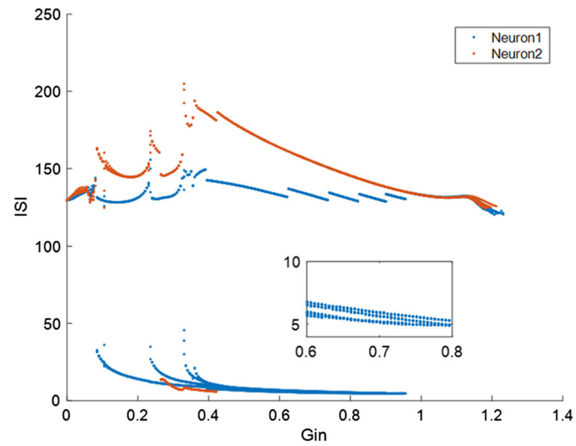

Fig. 3 Bifurcation diagram of neuronal firing ISI with different Inhibitory magnetic field coupling intensity, $I_{\text{ext}} = 1.8$; (the blue is the response of the first neuron, and the orange is the response of the second neuron) The inserted figure is an enlarged version

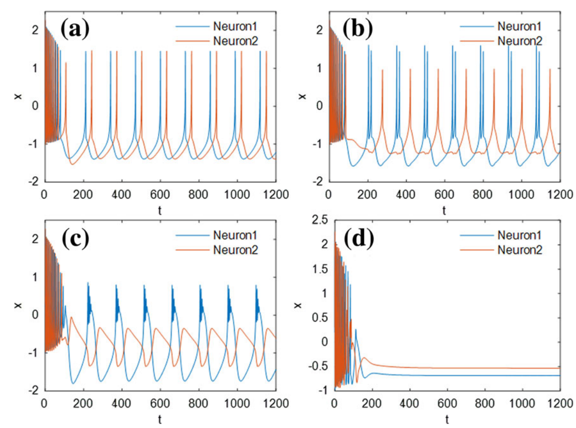

Fig. 4 Sampled time series for membrane potential, $I_{\text{ext}} = 1.8$ (the blue is the response of the first neuron, and the orange is the response of the second neuron). **a** $G_{\text{in}} = 0$; **b** $G_{\text{in}} = 0.2$; **c** $G_{\text{in}} = 0.8$; **d** $G_{\text{in}} = 2$

It has been discovered that changing the magnetic coupling strength alters the firing mode of neurons. With the increase of magnetic field coupling intensity, the firing mode of neuron 1 becomes more and more complex, and the observed spikes become more and more intensive. To observe the bifurcation diagram in greater detail, zoom in on the bifurcation diagram near $G_{\text{in}} = 0.8$. The neuron starts to inhibit the firing until the magnetic field coupling intensity reaches a certain degree. We can find that the bifurcation diagram disap-

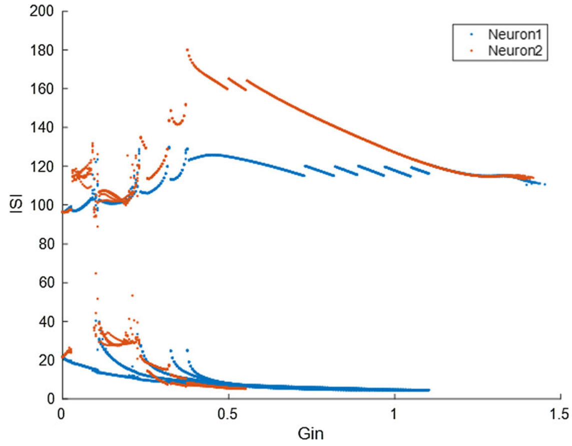

Fig. 5 Bifurcation diagram of neuronal firing ISI with different Inhibitory magnetic field coupling intensity, $I_{\text{ext}} = 2.3$ (the blue is the response of the first neuron, and the orange is the response of the second neuron)

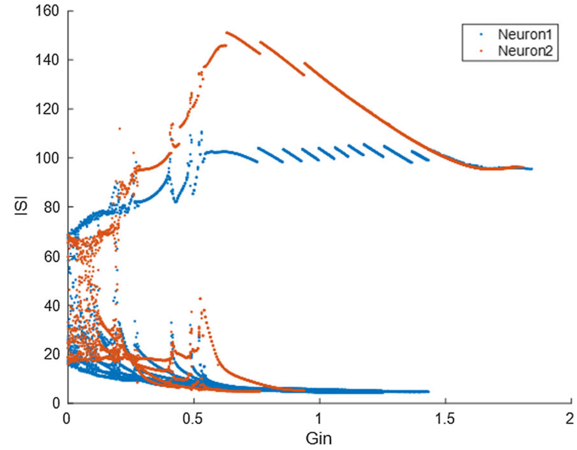

Fig. 7 Bifurcation diagram of neuronal firing ISI with different Inhibitory magnetic field coupling intensity, $I_{\text{ext}} = 3.2$ (the blue is the response of the first neuron, and the orange is the response of the second neuron)

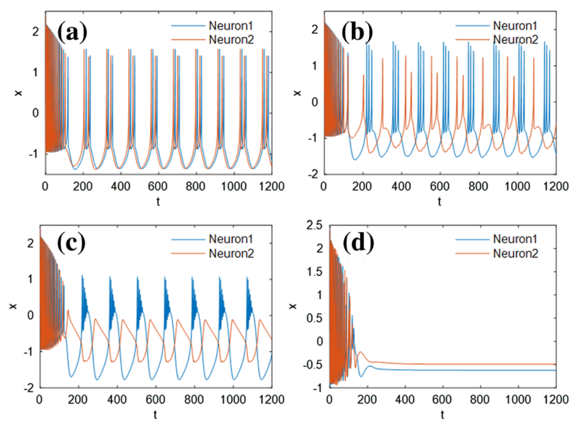

Fig. 6 Sampled time series for membrane potential, $I_{\text{ext}} = 2.3$ (the blue is the response of the first neuron, and the orange is the response of the second neuron). **a** $G_{\text{in}} = 0$; **b** $G_{\text{in}} = 0.2$; **c** $G_{\text{in}} = 0.8$; **d** $G_{\text{in}} = 2$

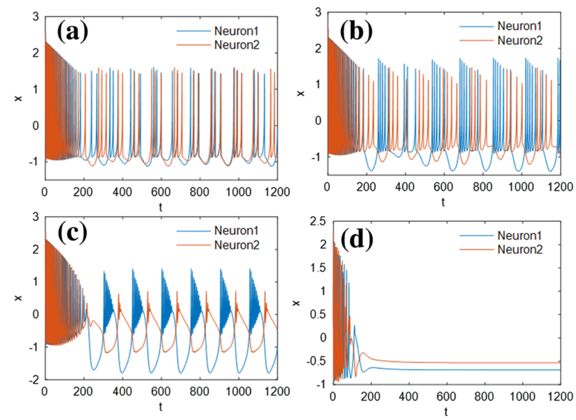

Fig. 8 Sampled time series for membrane potential, $I_{\text{ext}} = 3.2$ (the blue is the response of the first neuron, and the orange is the response of the second neuron). **a** $G_{\text{in}} = 0$; **b** $G_{\text{in}} = 0.2$; **c** $G_{\text{in}} = 0.8$; **d** $G_{\text{in}} = 2$

pears, indicating that the neuron is stationary. With the increase of magnetic coupling intensity, the amplitude and frequency of the membrane potential of neuron 2 became smaller and smaller and reached the quiescent state before neuron 1.

In case 2, the intensity of magnetic field coupling was changed to detect the influence of magnetic field coupling on neuron firing mode. The bifurcation diagram of ISI and the time series diagram are shown in Figs. 5 and 6.

With the increase of excitation current, more inhibitory magnetic field coupling is needed to make the neuron reach the quiescent state. The different discharge patterns of the two neurons were observed. The two neurons move from the same firing mode to a different one due to inhibitory magnetic coupling. Figure 6 shows the existence of burst discharge and Subthreshold oscillation [57] and the existence of burst discharge and chaotic state. Moreover, when the neuron is stationary, the membrane potential of neuron 1 is lower than that of neuron 2.

In case 3, two neurons with different initial values at chaotic discharge were selected to change the intensity of magnetic field coupling, and the effect of magnetic field coupling on neuron firing mode was detected. Bifurcation of ISI with parameter G_{in} and neuron firing patterns are shown in Figs. 7 and 8.

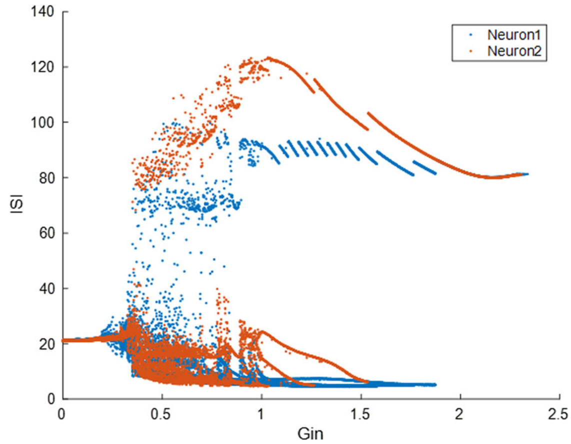

Fig. 9 Bifurcation diagram of neuronal firing ISI with different Inhibitory magnetic field coupling intensity, $I_{\text{ext}} = 4$ (the blue is the response of the first neuron, and the orange is the response of the second neuron)

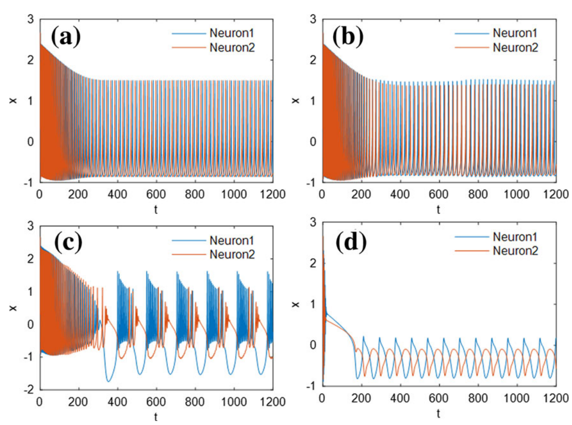

Fig. 10 Sampled time series for membrane potential, $I_{\text{ext}} = 4$(the blue is the response of the first neuron, and the orange is the response of the second neuron). **a** $G_{\text{in}} = 0$; **b** $G_{\text{in}} = 0.2$; **c** $G_{\text{in}} = 0.8$; **d** $G_{\text{in}} = 2$

As seen from the diagram, neurons can have a variety of discharge modes by adjusting the magnetic field coupling intensity. With the increase of magnetic field coupling intensity, the discharge modes of the two neurons change from chaos state to burst state and period-1 discharge and static form.

In case 4, two neurons at periodic oscillation were selected to change the intensity of magnetic field coupling, and the effect of magnetic field coupling on neuron firing mode was detected. Bifurcation of ISI with parameter G_{in} and neuron firing patterns are shown in Figs. 9 and 10.

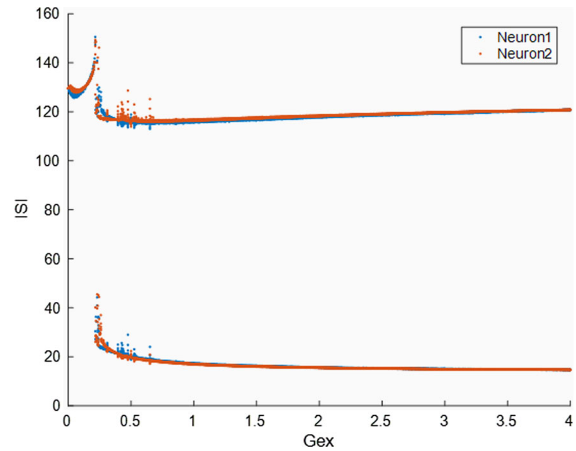

Fig. 11 Bifurcation diagram of neuronal firing ISI with different excitatory magnetic field coupling intensity, $I_{\text{ext}} = 1.8$ (the blue is the response of the first neuron, and the orange is the response of the second neuron)

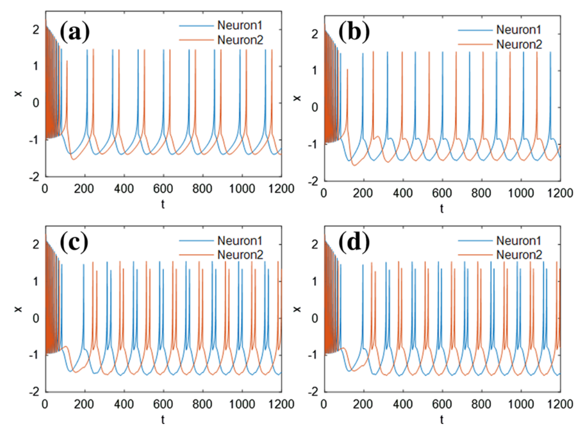

Fig. 12 Sampled time series for membrane potential, $I_{\text{ext}} = 1.8$ (the blue is the response of the first neuron, and the orange is the response of the second neuron). **a** $G_{\text{ex}} = 0$; **b** $G_{\text{ex}} = 0.2$; **c** $G_{\text{ex}} = 0.8$; **d** $G_{\text{ex}} = 2$

The discharge mode can be controlled by selecting suitable magnetic coupling intensity. The two neurons move from the same firing mode to a different one due to inhibitory magnetic coupling. When $G_{\text{in}} = 2$, the neuron firing pattern is subthreshold oscillation rather than resting, as shown in Fig. 10d. And with the increase of external stimulus current, the two neurons need more inhibitory magnetic coupling strength to reach the resting state.

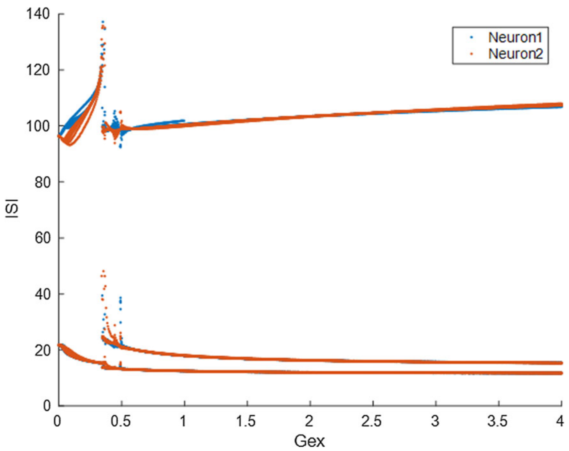

Fig. 13 Bifurcation diagram of neuronal firing ISI with different excitatory magnetic field coupling intensity, $I_{\text{ext}} = 2.3$ (the blue is the response of the first neuron, and the orange is the response of the second neuron)

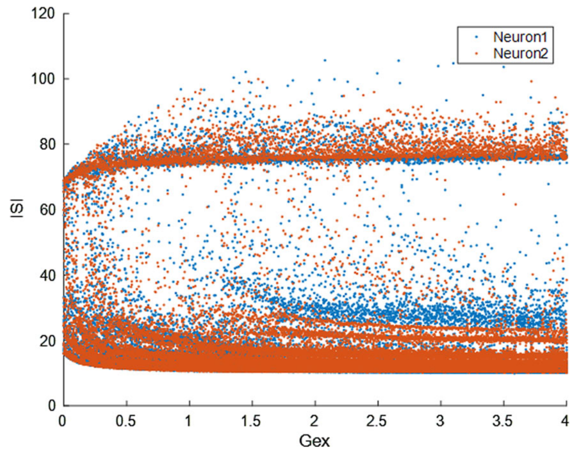

Fig. 15 Bifurcation diagram of neuronal firing ISI with different excitatory magnetic field coupling intensity, $I_{\text{ext}} = 3.2$ (the blue is the response of the first neuron, and the orange is the response of the second neuron)

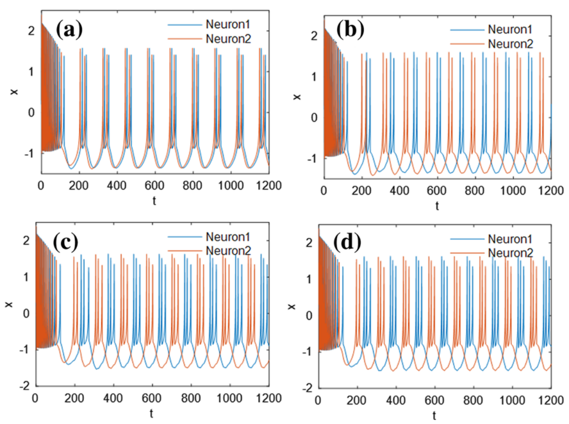

Fig. 14 Sampled time series for membrane potential, $I_{\text{ext}} = 2.3$ (the blue is the response of the first neuron, and the orange is the response of the second neuron). **a** $G_{\text{ex}} = 0$; **b** $G_{\text{ex}} = 0.2$; **c** $G_{\text{ex}} = 0.8$; **d** $G_{\text{ex}} = 2$

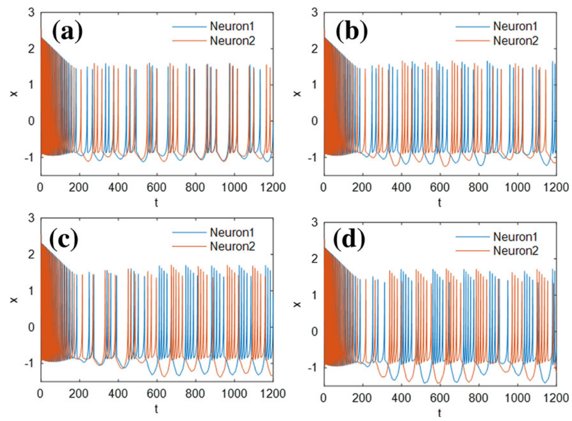

Fig. 16 Sampled time series for membrane potential, $I_{\text{ext}} = 3.2$ (the blue is the response of the first neuron, and the orange is the response of the second neuron). **a** $G_{\text{ex}} = 0$; **b** $G_{\text{ex}} = 0.2$; **c** $G_{\text{ex}} = 0.8$; **d** $G_{\text{ex}} = 2$

3.2 Excitatory magnetic field coupling

In case 1, two neurons with peak discharge were stimulated by an excitatory coupling magnetic field. Then the coupling intensity was changed to observe the firing of the neurons without synaptic coupling; the results are presented in Figs. 11 and 12.

With the increase of magnetic coupling intensity, the two neurons' firing mode becomes more and more complex, and the observed spikes become denser. The firing mode of neurons changes from peak discharge to period-2 discharge.

In case 2, two neurons with burst discharge were stimulated by an excitatory coupling magnetic field. Then the coupling intensity was changed to observe the neurons firing without synaptic coupling. The results are presented in Figs. 13 and 14.

Neurons firing in period-2 discharge flip to firing in a period-3 discharge after being activated by an excitatory magnetic coupling. And it was found that excitatory magnetic fields made neurons asynchronous.

In case 3, two neurons with chaotic discharge were stimulated by an excitatory coupling magnetic field, and then the coupling intensity was changed to observe the discharge of the neurons without synaptic coupling. The results are presented in Figs. 15 and 16.

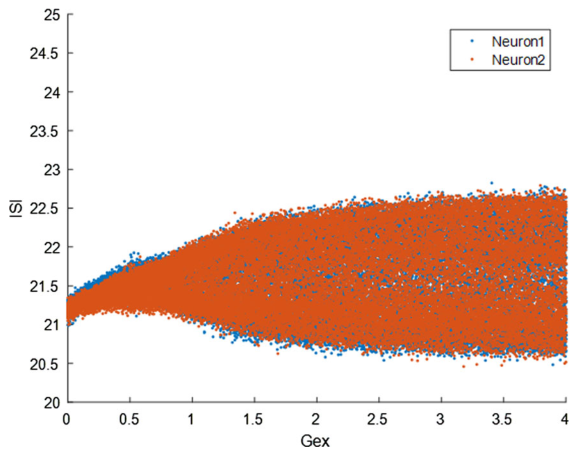

Fig. 17 Bifurcation diagram of neuronal firing ISI with different excitatory magnetic field coupling intensity, $I_{ext} = 4$ (the blue is the response of the first neuron, and the orange is the response of the second neuron)

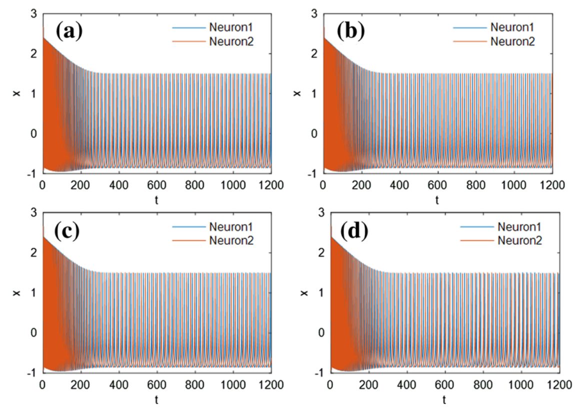

Fig. 18 Sampled time series for membrane potential, $I_{ext} = 4$ (the blue is the response of the first neuron, and the orange is the response of the second neuron). **a** $G_{ex} = 0$; **b** $G_{ex} = 0.2$; **c** $G_{ex} = 0.8$; **d** $G_{ex} = 2$

The bifurcation diagram shows that the two neurons are in chaotic discharge, but through the sequence diagram, we can find that the excitatory magnetic coupling promotes the neuron discharge.

In case 4, two neurons with Periodic oscillation were stimulated by an excitatory coupling magnetic field, and then the coupling intensity was changed to observe the discharge of the neurons without synaptic coupling. The results are presented in Figs. 17 and 18.

In conclusion, the effects of excitatory and inhibitory magnetic field coupling on neuron discharge differ. Excitatory magnetic field coupling can benefit neuron firing but also affect neuron firing patterns, complicating electrical activity. Inhibitory magnetic field coupling can enhance neuron firing when the coupling intensity is small but can inhibit neuron firing

Table 3 Different ways to couple HR neurons

Different coupling	Equations	Remarks
Excitatory electrical synaptic [55]	$\begin{cases}\dot{x}_1 = f(x_1, p) + D(x_2 - x_1)\\ \dot{\varphi}_1 = k_1x_1 - k_2\varphi_1\\ \dot{x}_2 = f(x_2, p) + D(x_1 - x_2)\\ \dot{\varphi}_2 = k_1x_2 - k_2\varphi_2,\end{cases}$	Bidirectional, electric field
Excitatory chemical synaptic [58]	$\begin{cases}\dot{x}_1 = f(x_1, p)\\ \dot{\varphi}_1 = k_1x_1 - k_2\varphi_1\\ \dot{x}_2 = f(x_2, p) + g_{ex}(v_{se} - x_2)(\frac{1}{1+e^{(-\lambda(x_1(t-\tau_c)-\theta))}}) \quad v_{se} > x_{2\max}\\ \dot{\varphi}_2 = k_1x_2 - k_2\varphi_2,\end{cases}$	Unidirectional, time delay, neurotransmitter
Inhibitory chemical synaptic [58]	$\begin{cases}\dot{x}_1 = f(x_1, p)\\ \dot{\varphi}_1 = k_1x_1 - k_2\varphi_1\\ \dot{x}_2 = f(x_2, p) + g_{in}(v_{se} - x_2)(\frac{1}{1+e^{(-\lambda(x_1(t-\tau_c)-\theta))}}) \quad v_{se} < x_{2\min}\\ \dot{\varphi}_2 = k_1x_2 - k_2\varphi_2,\end{cases}$	Unidirectional, time delay, neurotransmitter
Excitatory magnetic field [2]	$\begin{cases}\dot{x}_1 = f(x_1, p)\\ \dot{\varphi}_1 = k_1x_1 - k_2\varphi_1 + G_{ex}(\varphi_2 - \varphi_1)\\ \dot{x}_2 = f(x_2, p)\\ \dot{\varphi}_2 = k_1x_2 - k_2\varphi_2 + G_{ex}(\varphi_1 - \varphi_2),\end{cases}$	Bidirectional, magnetic field
Inhibitory magnetic field	$\begin{cases}\dot{x}_1 = f(x_1, p)\\ \dot{\varphi}_1 = k_1x_1 - k_2\varphi_1 - G_{in}(\varphi_2 + \varphi_1)\\ \dot{x}_2 = f(x_2, p)\\ \dot{\varphi}_2 = k_1x_2 - k_2\varphi_2 + G_{in}(\varphi_1 + \varphi_2),\end{cases}$	Bidirectional, magnetic field

when the coupling intensity is vital. The neurons enter a static state when the magnetic coupling strength reaches a critical point. As the external stimulus current increases, more inhibitory magnetic field coupling strength is required to make the neuron enter the quiescent state.

4 Conclusions

Sequences of spikes carry out the information of neurons; neurons can modulate the firing patterns of other neurons using magnetic fields. Like synapses, magnetic coupling acts as a means of transmitting data between neurons. Thus, the magnetic coupling may have properties similar to synaptic coupling. This paper divided the magnetic field coupling into excitation and inhibition magnetic field coupling, and two coupling models are established, respectively. The method of transmitting neuron information through magnetic field coupling is further improved. It increases the magnetic coupling strength of the excitatory model, which promotes neuronal electrical activity. A high enough inhibitory magnetic coupling causes the neuron to become quiescent. Table 3 lists the two neurons' synaptic and magnetic coupling models. Chemical synaptic coupling is unidirectional; information can only be transmitted from the presynaptic neuron to the postsynaptic neuron. Chemical synapses have a time delay due to synaptic cleft. Magnetic coupling is the ability of neurons to interact with each other. It is bi-directional and has no time delay. It is divided into excitatory synapses and inhibitory synapses. Moreover, the neuronal magnetic field not only affects postsynaptic neurons but also has a diffusion effect. Because neurons are exposed to the integrated magnetic fields of other neurons, the next step of this paper is to study the interaction of magnetic fields of multiple neurons.

Data availability The datasets generated during and/or analyzed during the current study are available from the corresponding author on reasonable request.

Declarations

Funding This work is supported by the National Natural Science Foundation of China (No. 61971185) and Natural Science Foundation of Hunan Province (2020JJ4218).

Conflict of interest The authors declare that they have no conflicts of interest.

References

1. Komendantov, A.O., Venkadesh, S., Rees, C.L., Wheeler, D.W., Hamilton, D.J., Ascoli, G.A.: Quantitative firing pattern phenotyping of hippocampal neuron types. Sci. Rep. **9**(1), 1–17 (2019)
2. Ma, J., Tang, J.: A review for dynamics in neuron and neuronal network. Nonlinear Dyn. **89**(3), 1569–1578 (2017)
3. Chua, L.: Memristor—the missing circuit element. IEEE Trans. Circuit Theory **18**(5), 507–519 (1971)
4. Ma, M., Yang, Y., Qiu, Z., Peng, Y., Sun, Y., Li, Z., Wang, M.: A locally active discrete memristor model and its application in a hyperchaotic map. Nonlinear Dyn. **66**, 1–15 (2022)
5. Ma, X., Mou, J., Xiong, L., Banerjee, S., Cao, Y., Wang, J.: A novel chaotic circuit with coexistence of multiple attractors and state transition based on two memristors. Chaos Solitons Fract. **152**, 111363 (2021)
6. Lin, H., Wang, C., Hong, Q., Sun, Y.: A multi-stable memristor and its application in a neural network. IEEE Trans. Circuits Syst. II Express Briefs **67**(12), 3472–3476 (2020)
7. Zhang, S., Zheng, J., Wang, X., Zeng, Z.: A novel no-equilibrium hr neuron model with hidden homogeneous extreme multistability. Chaos Solitons Fract. **145**, 110761 (2021)
8. Varshney, V., Sabarathinam, S., Prasad, A., Thamilmaran, K.: Infinite number of hidden attractors in memristor-based autonomous duffing oscillator. Int. J. Bifurc. Chaos **28**(01), 1850013 (2018)
9. Deng, Q., Wang, C., Yang, L.: Four-wing hidden attractors with one stable equilibrium point. Int. J. Bifurc. Chaos **30**(06), 2050086 (2020)
10. Lin, H., Wang, C., Cui, L., Sun, Y., Xu, C., Yu, F.: Brain-like initial-boosted hyperchaos and application in biomedical image encryption. IEEE Trans. Ind. Inform. (2022). https://doi.org/10.1109/TII.2022.3155599
11. Zhou, L., Wang, C., Zhou, L.: Generating hyperchaotic multi-wing attractor in a 4d memristive circuit. Nonlinear Dyn. **85**(4), 2653–2663 (2016)
12. Zhou, L., Wang, C., Zhou, L.: A novel no-equilibrium hyperchaotic multiwing system via introducing memristor. Int. J. Circuit Theory Appl. **46**(1), 84–98 (2018)
13. Yan, D., Wang, L., Duan, S., Chen, J., Chen, J.: Chaotic attractors generated by a memristor-based chaotic system and Julia fractal. Chaos Solitons Fract. **146**, 110773 (2021)
14. Lin, H., Wang, C., Yu, F., Xu, C., Hong, Q., Yao, W., Sun, Y.: An extremely simple multiwing chaotic system: Dynamics analysis, encryption application, and hardware implementation. IEEE Trans. Ind. Electron. **68**(12), 12708–12719 (2021)
15. Yu, F., Kong, X., Chen, H., Yu, Q., Cai, S., Huang, Y., Du, S.: A 6d fractional-order memristive Hopfield neural network and its application in image encryption. Front. Phys. **109**, 66 (2022)
16. Yang, Y., Wang, L., Duan, S., Luo, L.: Dynamical analysis and image encryption application of a novel memristive hyperchaotic system. Opt. Laser Technol. **133**, 106553 (2021)
17. Lin, H., Wang, C., Chen, C., Sun, Y., Zhou, C., Xu, C., Hong, Q.: Neural bursting and synchronization emulated by neural

networks and circuits. IEEE Trans. Circuits Syst. I Regul. Pap. **68**(8), 3397–3410 (2021)

18. Xu, C., Wang, C., Jiang, J., Sun, J., Lin, H.: Memristive circuit implementation of context-dependent emotional learning network and its application in multi-task. IEEE Trans. Comput. Aided Des. Integr. Circuits Syst. **66**, 1 (2021)
19. Yang, L., Wang, C.: Emotion model of associative memory possessing variable learning rates with time delay. Neurocomputing **460**, 117–125 (2021)
20. Lin, H., Wang, C., Deng, Q., Xu, C., Deng, Z., Zhou, C.: Review on chaotic dynamics of memristive neuron and neural network. Nonlinear Dyn. **106**(1), 959–973 (2021)
21. Xie, W., Wang, C., Lin, H.: A fractional-order multistable locally active memristor and its chaotic system with transient transition, state jump. Nonlinear Dyn. **104**(4), 4523–4541 (2021)
22. Chen, J., Li, C., Huang, T., Yang, X.: Global stabilization of memristor-based fractional-order neural networks with delay via outputfeedback control. Mod. Phys. Lett. B **31**(05), 1750031 (2017)
23. Jahanshahi, H., Yousefpour, A., Munoz-Pacheco, J.M., Kacar, S., Pham, V.-T., Alsaadi, F.E.: A new fractional-order hyperchaotic memristor oscillator: Dynamic analysis, robust adaptive synchronization, and its application to voice encryption. Appl. Math. Comput. **383**, 125310 (2020)
24. Lin, H., Wang, C., Sun, Y., Yao, W.: Firing multistability in a locally active memristive neuron model. Nonlinear Dyn. **100**(4), 3667–3683 (2020)
25. Li, C., Li, H., Xie, W., Du, J.: A s-type bistable locally active memristor model and its analog implementation in an oscillator circuit. Nonlinear Dyn. **106**(1), 1041–1058 (2021)
26. Dong, Y., Wang, G., Iu, H.H.-C., Chen, G., Chen, L.: Coexisting hidden and self-excited attractors in a locally active memristor-based circuit. Chaos Interdiscip. J. Nonlinear Sci. **30**(10), 103123 (2020)
27. Lv, M., Wang, C., Ren, G., Ma, J., Song, X.: Model of electrical activity in a neuron under magnetic flow effect. Nonlinear Dyn. **85**(3), 1479–1490 (2016)
28. Lv, M., Ma, J.: Multiple modes of electrical activities in a new neuron model under electromagnetic radiation. Neurocomputing **205**, 375–381 (2016)
29. Bao, H., Liu, W., Chen, M.: Hidden extreme multistability and dimensionality reduction analysis for an improved non-autonomous memristive Fitzhugh–Nagumo circuit. Nonlinear Dyn. **96**(3), 1879–1894 (2019)
30. Bao, H., Hu, A., Liu, W., Bao, B.: Hidden bursting firings and bifurcation mechanisms in memristive neuron model with threshold electromagnetic induction. IEEE Trans. Neural Netw. Learn. Syst. **31**(2), 502–511 (2019)
31. Ma, J., Zhang, G., Hayat, T., Ren, G.: Model electrical activity of neuron under electric field. Nonlinear Dyn. **95**(2), 1585–1598 (2019)
32. Yan, B., Panahi, S., He, S., Jafari, S.: Further dynamical analysis of modified Fitzhugh–Nagumo model under the electric field. Nonlinear Dyn. **101**(1), 521–529 (2020)
33. Wu, F., Ma, J., Zhang, G.: A new neuron model under electromagnetic field. Appl. Math. Comput. **347**, 590–599 (2019)
34. Lu, L., Jia, Y., Xu, Y., Ge, M., Yang, L., Zhan, X.: Energy dependence on modes of electric activities of neuron driven by different external mixed signals under electromagnetic induction. Sci. China Technol. Sci. **62**(3), 427–440 (2019)
35. Hindmarsh, J., Rose, R.: A model of the nerve impulse using two first-order differential equations. Nature **296**(5853), 162–164 (1982)
36. Gambuzza, L.V., Di Patti, F., Gallo, L., Lepri, S., Romance, M., Criado, R., Frasca, M., Latora, V., Boccaletti, S.: Stability of synchronization in simplicial complexes. Nat. Commun. **12**(1), 1–13 (2021)
37. Wang, G., Xu, Y., Ge, M., Lu, L., Jia, Y.: Mode transition and energy dependence of Fitzhugh–Nagumo neural model driven by high-low frequency electromagnetic radiation. AEU Int. J. Electron. Commun. **120**, 153209 (2020)
38. FitzHugh, R.: Impulses and physiological states in theoretical models of nerve membrane. Biophys. J. **1**(6), 445–466 (1961)
39. Yang, Y., Ma, J., Xu, Y., Jia, Y.: Energy dependence on discharge mode of Izhikevich neuron driven by external stimulus under electromagnetic induction. Cognit. Neurodyn. **15**(2), 265–277 (2021)
40. Izhikevich, E.: Simple model of spiking neurons. IEEE Trans. Neural Netw. **14**(6), 1569–1572 (2003)
41. Wan, Q., Yan, Z., Li, F., Liu, J., Chen, S.: Multistable dynamics in a Hopfield neural network under electromagnetic radiation and dual bias currents. Nonlinear Dyn. **66**, 1–17 (2022)
42. Wan, Q., Yan, Z., Li, F., Chen, S., Liu, J.: Complex dynamics in a Hopfield neural network under electromagnetic induction and electromagnetic radiation. Chaos Interdiscip. J. Nonlinear Sci. **32**(7), 073107 (2022)
43. Lin, H., Wang, C.: Influences of electromagnetic radiation distribution on chaotic dynamics of a neural network. Appl. Math. Comput. **369**, 124840 (2020)
44. Yu, F., Zhang, Z., Shen, H., Huang, Y., Cai, S., Jin, J., Du, S.: Design and fpga implementation of a pseudo-random number generator based on a Hopfield neural network under electromagnetic radiation. Front. Phys. **9**, 302 (2021)
45. Lin, H., Wang, C., Yao, W., Tan, Y.: Chaotic dynamics in a neural network with different types of external stimuli. Commun. Nonlinear Sci. Numer. Simul. **90**, 105390 (2020)
46. Qu, L., Du, L., Hu, H., Cao, Z., Deng, Z.: Pattern control of external electromagnetic stimulation to neuronal networks. Nonlinear Dyn. **102**(4), 2739–2757 (2020)
47. Zandi-Mehran, N., Jafari, S., Hashemi Golpayegani, S.M.R., Nazarimehr, F., Perc, M.: Different synaptic connections evoke different firing patterns in neurons subject to an electromagnetic field. Nonlinear Dyn. **100**(2), 1809–1824 (2020)
48. Alcamí, P., Pereda, A. E.: Beyond plasticity: the dynamic impact of electrical synapses on neural circuits. Nat. Rev. Neurosci. **20**(5), 253–271 (2019)
49. Xu, K., Maidana, J.P., Orio, P.: Diversity of neuronal activity is provided by hybrid synapses. Nonlinear Dyn. **105**(3), 2693–2710 (2021)
50. Li, Y., Gu, H., Jia, B., Ding, X.: The nonlinear mechanism for the same responses of neuronal bursting to opposite self-feedback modulations of autapse. Sci. China Technol. Sci. **64**(7), 1459–1471 (2021)
51. Uzuntarla, M.: Firing dynamics in hybrid coupled populations of bistable neurons. Neurocomputing **367**, 328–336 (2019)

52. Ma, J., Mi, L., Zhou, P., Xu, Y., Hayat, T.: Phase synchronization between two neurons induced by coupling of electromagnetic field. Appl. Math. Comput. **307**, 321–28 (2017)
53. Guo, S., Xu, Y., Wang, C., Jin, W., Hobiny, A., Ma, J.: Collective response, synapse coupling and field coupling in neuronal network. Chaos Solitons Fract. **105**, 120–127 (2017)
54. Zhao, Y., Sun, X., Liu, Y., Kurths, J.: Phase synchronization dynamics of coupled neurons with coupling phase in the electromagnetic field. Nonlinear Dyn. **93**(3), 1315–1324 (2018)
55. Zhou, Q., Wei, D.Q.: Collective dynamics of neuronal network under synapse and field coupling. Nonlinear Dyn. **105**(1), 753–765 (2021)
56. Xu, Y., Jia, Y., Ma, J., Hayat, T., Alsaedi, A.: Collective responses in electrical activities of neurons under field coupling. Sci. Rep. **8**(1), 1–10 (2018)
57. Ozer, M., Uzuntarla, M., Agaoglu, S.N.: Effect of the subthreshold periodic current forcing on the regularity and the synchronization of neuronal spiking activity. Phys. Lett. A **360**(1), 135–140 (2006)
58. Rakshit, S., Bera, B.K., Ghosh, D., Sinha, S.: Emergence of synchronization and regularity in firing patterns in timevarying neural hypernetworks. Phys. Rev. E **97**, 052304 (2018)